Solution Structure of Synbindin Atypical PDZ Domain and Interaction with Syndecan-2

Shilong Fan[1,2,†], Yingang Feng[2,3,4,†], Zhiyi Wei[1,2], Bin Xia[3,4,5,*] and Weimin Gong[1,2,*]

[1]*School of Life Sciences, University of Science and Technology of China, Hefei, Anhui, 230026, P.R. China;* [2]*National Laboratory of Biomacromolecules, Center for Structural and Molecular Biology, Institute of Biophysics, Chinese Academy of Sciences, Beijing, 100101, P.R. China;* [3]*Beijing Nuclear Magnetic Resonance Center,* [4]*College of Chemistry and Molecular Engineering,* [5]*College of Life Science Peking University, Beijing, 100871, P.R. China*

Abstract: Synbindin is one component of Transport protein particle (TRAPP) complexes. In the hippocampal neurons, synbindin binds syndecan-2 by its atypical PDZ domain (APD) and may regulate the formation of dendritic spines. To investigate the interaction of synbindin and syndecan-2, we determined the solution structure of the synbindin APD by NMR. The structure of APD is different from the classical canonical PDZ domains by lacking the typical αA helix and the signature sequence Gly-ψ-Gly-ψ. These differences indicate that APD may not bind syndecan-2 with the typical binding mode of other PDZ domain proteins. In NMR titration experiments, APD do not bind with the C-terminal TKEFYA peptide of syndecan-2, but can interact with the 32-residue cytoplasmic domain of syndecan-2 very weakly.

Keywords: Synbindin, syndecan, PDZ domain, NMR, protein interaction.

INTRODUCTION

Transport protein particle (TRAPP) is a large multiprotein complex that involves in ER-to-Golgi and intra-Golgi traffic, which is found in both yeast and human [1,2]. In yeast, the BET3p, BET5p, Trs20p, Trs23p, Trs31p, Trs33p, Trs85p is common subunits in TRAPP I and TRAPP II, and Trs65p, Trs120p, Trs130p is additional subunits of TRAPP II. Synbindin is the human orthologue of yeast Trs23p. Although the molecular mechanism governing TRAPP-mediated protein transport is still largely unknown, recent structural studies of various components of the TRAPP complex have provided much needed insights into the mode of assembly and possible action mechanism of the TRAPP complexes [3-8].

Synbindin was first identified by a yeast two-hybrid screening using the syndecan-2 cytoplasmic domain as bait. In hippocampal neurons, synbindin can associate with the synaptic membrane through direct interaction of its atypical PDZ domain (APD) with Syndecan-2. It was further suggested that syndecan-2 induces spine formation by recruiting intracellular vesicles toward postsynaptic sites through the interaction with synbindin [9]. Syndecan-2 can interact with many PDZ-domain proteins through its C-terminal EFYA motif of syndecan-2, such as syntenin and synectin [10]. This typical binding mode was also suggested to be similar in the interaction of syndecan-2 and synbindin [9].

*Address correspondence to these authors at the School of Life Sciences, University of Science and Technology of China, Hefei, Anhui, 230026, P.R. China; National Laboratory of Biomacromolecules, Center for Structural and Molecular Biology, Institute of Biophysics, Chinese Academy of Sciences, Beijing, 100101, P.R. China; Beijing Nuclear Magnetic Resonance Center, Beijing, 100871, P.R. China; E-mails: wgong@ibp.ac.cn and binxia@pku.edu.cn

†*These authors contributed equally to this work.*

To investigate the interaction of synbindin and syndecan-2, we solved the solution structure of the atypical PDZ domain (APD) of synbindin by NMR spectroscopy and titrated the APD with syndecan-2 C-terminal peptides. We found the structure of APD lack some structural elements which are necessary for typical PDZ-domain-peptide interactions. These differences suggest that APD may not bind syndecan-2 with the typical binding mode of other PDZ domain proteins. In NMR titration experiments we found APD do not bind with the C-terminal TKEFYA peptide of syndecan-2, but can interact with the cytoplasmic domain of syndecan-2 very weakly.

MATERIALS AND METHODS

Protein Expression and Purification

The recombined atypical PDZ domain (residues 19-106) was constructed to pET-28 vector with an N terminal His_6-tag. Protein was expressed in *E. coli* BL21 (DE3) cells and purified by a Ni-affinity column followed a Superdex G-75 column. The uniformly $^{15}N/^{13}C$ labeled proteins were obtained by growing the cells in M9-minimal medium containing $^{15}NH_4Cl$ and ^{13}C-glucose as the sole nitrogen and carbon sources, respectively.

The peptides of syndecan-2 cytoplasmic domain (S2CD, 32 residues RMRKKDEGSYDLGERKPSSAAYQKAPTK EFYA) and the C-terminal peptide (S2CP, TKEFYA) were chemically synthesized (SciLight Biotechnology, LCC.) and their purities were >96% checked by HPLC and mass spectroscopy.

NMR Spectroscopy

Samples for NMR experiments contain 1~1.5 mM ^{13}C and ^{15}N-labeled protein and 50 mM potassium phosphate buffer at pH 6.0, 90%H_2O/10%D_2O, 0.01% sodium 2,2-

0929-8665/09 $55.00+.00

dimethylsilapentane-5-sulfonate (DSS), and 0.01% NaN_3. The samples also contain 50mM L-amino acids Arg and Glu for improving the solubility and stability [11].

All NMR experiments were carried at 293 K on a Bruker Avance 500 MHz spectrometer with a triple resonance cryoprobe. The NMR experiments for ^1H, ^{15}N, and ^{13}C resonance assignments include: 2D ^1H-^{15}N HSQC, ^1H-^{13}C HSQC, CB(CGCD)HD, 3D HNCA, HNCACB, CBCA(CO)NH, HNCO, HN(CA)CO, HBHA(CBCA)CONH, ^1H-^{15}N TOCSY-HSQC, HC(C)H-TOCSY, (H)CCH-TOCSY, and HC(C)H-COSY. Distance constrains were obtained from three NOE experiments with 120 ms mixing times: 3D ^{15}N NOESY-HSQC and ^{13}C NOESY-HSQC for aliphatic regions and aromatic regions. All NMR spectra were processed and analyzed using NMRPipe [12] and NMRView [13] respectively. Proton chemical shifts and ^{15}N and ^{13}C chemical shifts were referenced to internal DSS and indirectly to DSS respectively.

Initial structures of the synbindin atypical PDZ domain were generated using CYANA with restraints from the CANDID module [14]. These initial structures were then used as filter models for SANE [15] to obtain further NOE assignments, and the new distance restraints were then used for another round of CYANA calculation. Dihedral angle restraints and hydrogen bond restraints were also used for the structure calculation. Dihedral angle restraints were obtained using TALOS [16] while hydrogen bond restraints were added according to the secondary structures predicted based on chemical shifts and NOEs. When the lowest CYANA target function value was smaller than 0.5 $Å^2$ and the number of NOE violations was less than 5, a total of 200 structures were calculated using CYANA and the 100 structures with the lowest target function values were selected for refinement with AMBER 7 [17]. Again, SANE was used to assist NOE assignment. The final 20 structures with lowest AMBER energy were selected from 100 refined structures. The quality of the structures was analyzed with MOLMOL [18] and PROCHECK-NMR [19]. Restraints and structure statistics of the synbindin atypical PDZ domain are listed in Table **2**.

The interactions between the synbindin atypical PDZ domain and the S2CD or S2CP were detected by monitoring the chemical shift changes of the ^1H-^{15}N HSQC spectra of 0.4 mM ^{15}N labeled atypical PDZ domain titrated with the synthesized S2CD or S2CP. Powder of peptides was added to the APD solution to a proper molar ratio.

Protein Data Bank Accession Codes

The atomic coordinates of synbindin APD have been deposited in the RCSB Protein Data Bank with the accession codes 2JSN. The chemical shift assignments of APD have been deposited in the BioMagResBank with the accession code 15370.

RESULTS AND DISCUSSION

Solution Structure of Synbindin APD

The ^1H-^{15}N HSQC spectrum of synbindin APD displays well-dispersed NMR spectra (Fig. **1A**). After the assignments of almost all the peaks in the ^1H-^{15}N HSQC spectrum obtained, we found that several residues in APD (residues 28, 29, 36–39, 54–58, 97) did not show detectable peaks in NMR spectra. Most of these residues are either totally disordered or with side-chain invisible in the crystal structure of synbindin. These regions in APD are likely to be mobile both in solution and in the crystal. Based on the assignments and constraints obtained from NOE experiments, the structure of APD was determined to high quality (Fig. **1B** and Table **1**).

The APD structure consists of six β-strands and one α-helix (Fig. **1C**). As see in canonical PDZ domains, the six β-strands form a β-barrel with the α-helix ($\alpha1_P$) located on one side of the β-barrel. The structural similarity between the APD and other PDZ domains is confirmed by structural similarity searches in the Protein Data Bank (PDB) by DALI [20] and SSM [21]. The PDZ domains (PDZ1 and PDZ2) of syntenin [22] and the first PDZ domain of NHERF (Na^+/H^+ exchange regulatory factor) [23] came out as having the closest structural similarities in the search. The overall RMSD (root mean square deviation) is larger than 2.5 Å between the APD and the three most similar PDZ domains, in contrast to ~ 1 Å between any pairs of the three canonical PDZ domains, indicating that the APD of synbindin is a rather unusual PDZ domain. Specifically, the APD of synbindin lacks the αA helix found in all known canonical PDZ domains. In contrast to canonical PDZ domains, the $\beta3_P/\beta4_P$-connecting sequence in the synbindin APD is very short (10 residues) and are largely flexible (Supp. Fig. **1**). The only helix $\alpha1_P$ of the APD corresponds to the αB helix in the canonical PDZ domain (Supp. Fig. **1**). However, the $\alpha1_P$ of APD is significantly shorter (6 residues) than those in majority of PDZ domains with known structures, although several PDZ domains with slightly short αB helix are also observed (e.g., PDZ2 of X11 and PDZ2 of syntenin). The position of the first residue in the $\alpha1_P$ of APD is miss-aligned for binding to the amino acid residues at the -2 position of canonical PDZ-binding carboxyl peptide. Canonical PDZ domains contain a signature motif with "Gly-ψ-Gly-ψ" sequence ('ψ' standing for a hydrophobic residue) in the βA and βB loop (corresponding to the $\beta1_P$ and $\beta2_P$ loop in the APD) (Supp. Fig. **1B**) [24]. The second Gly in the "Gly-ψ-Gly-ψ" motif is one of the most conserved residue in PDZ domains and is absolutely required for PDZ domains to bind its targets [25]. In APD, the second Gly in this signature motif is replaced by an Asp residue (Supp. Fig. **1**). Taken together, the atypical structural features of APD lead a prediction that the APD of synbindin may not function as a carboxyl peptide binder.

In addition, although with low sequence homology, the structure based sequence alignment shows some conserved hydrophobic residues between the APD of synbindin and other PDZ domains throughout the amino acid sequence (Supp. Fig. **1**). These hydrophobic residues interdigitate to form a hydrophobic core, which should be essential for stabilizing the PDZ fold. The result gives out a strong explanation of a character of PDZ domains, the divergence sequence similarity with the conservation PDZ fold accordingly.

Interactions Between Synbindin APD and Syndecan-2 by NMR Titration

Since syndecan-2 interacts with other PDZ-domain proteins by the C-terminal peptide EFYA, we titrated APD by a

Table 1. Restraints and Structure Statistics of the Synbindin Atypical PDZ Domain

Conformational restraints				
NOE restraints		2233		
	Intra-residue	665		
	Sequential	450		
	Medium	191		
	Long-range	381		
	Ambiguous	546		
Dihedral angle restraints		62		
	phi	31		
	psi	31		
Hydrogen bond restraints		20		
Chirality restraints		327		
	Omega angle	95		
	Side-chain	232		
Structure statistics of final 20 conformers				
Violations		Numbers	Maximum violation	
	Distance restraints	7	0.185 Å	
	Dihedral angle restraints	0		
RMSD		All residues [a]	Regular secondary structure [b]	
	Backbone heavy atoms	0.93	0.41	
	All heavy atoms	1.65	1.05	
PROCHECK				
	Most favored regions (%)	79.8		
	Additionally allowed regions (%)	18.6		
	Generously allowed regions (%)	1.0		
	Disallowed regions (%)	0.6 [c]		

[a] The flexible regions 11-25 and 102-106 are excluded.
[b] Residues 31-34, 39-43, 46-51, 62-66, 69-72, 75-76, 82-87, 93-99.
[c] These residues are in flexible regions without NMR signals.

synthesized syndecan-2 C-terminal peptide (S2CP) TKEFYA. However, no significant chemical shift change was observed in the ^{1}H-^{15}N HSQC spectra (Supp. Fig. **2**). It suggests that the APD does not bind with the S2CP, or bind with a very low affinity beyond the NMR detection. This is in agreement with the APD features of lacking key structural elements to binding a carboxyl peptide.

The observation that APD do not bind S2CP raised the question that how syndecan-2 interact with synbindin. We further titrated synbindin APD by the syndecan-2 cytoplasmic domain (S2CD), the C-terminal 32-residues peptide. Some peaks were shifted in the 2D ^{1}H-^{15}N HSQC spectrum of ^{15}N labeled APD (Fig. **2A**), indicating that the APD binds with the S2CD *in vitro*. The most significant shifted NH peaks are from four residues, His43, Asp44, Glu45, and Leu48, which are all located on the β-hairpin formed by $\beta2_P$ and $\beta3_P$ (Fig. **2B**), and the nearby residues also have small shifts (Fig. **2A**). This binding region of APD with S2CD is different from the typical binding site on PDZ domain with a carboxyl peptide (Fig. **2B**). These results suggest that the APD interacts with an internal sequence of the S2CD but not the "EFYA" tail. In addition, comparing with the affinity of syntenin PDZ domains and its ligand "TNEFYA" [26], the interactions between the APD and the S2CD are rather weak because of fewer NH signals affected and smaller chemical-

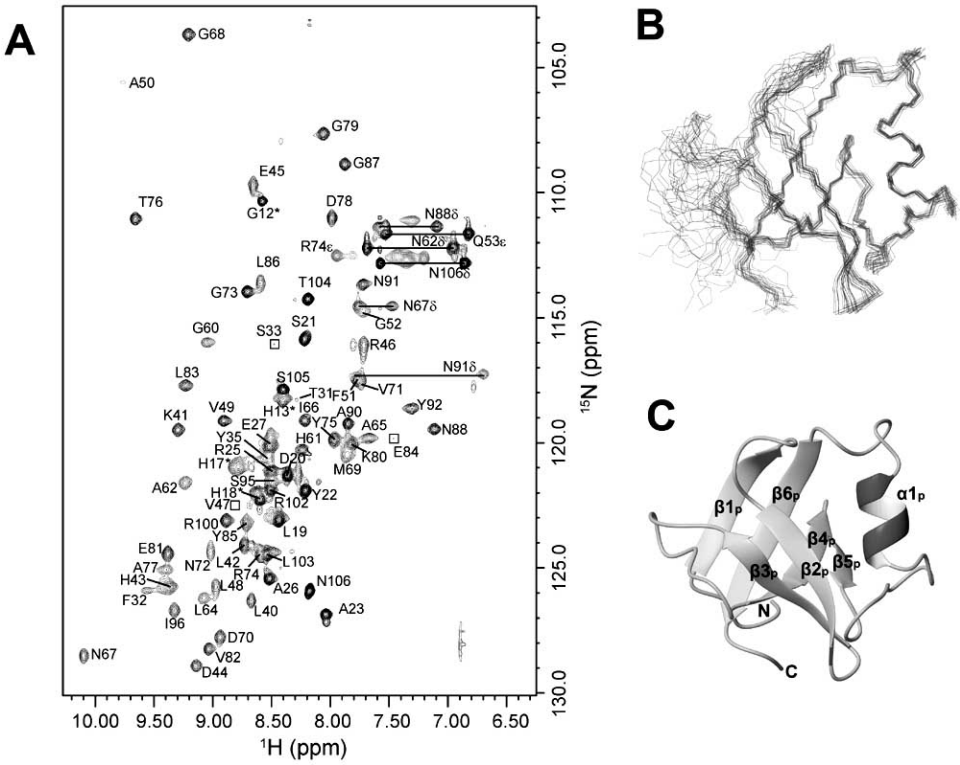

Figure 1. Solution structure of synbindin APD. (A) The ^{1}H-^{15}N HSQC spectrum of synbindin APD. Peaks are labeled with one-letter residue names and numbers. **(B)** Backbone ensemble of the twenty structures. **(C)** Ribbon representation of the structure. For clarity, only residues 25-102 of NMR structures are shown since the other residues are unstructured.

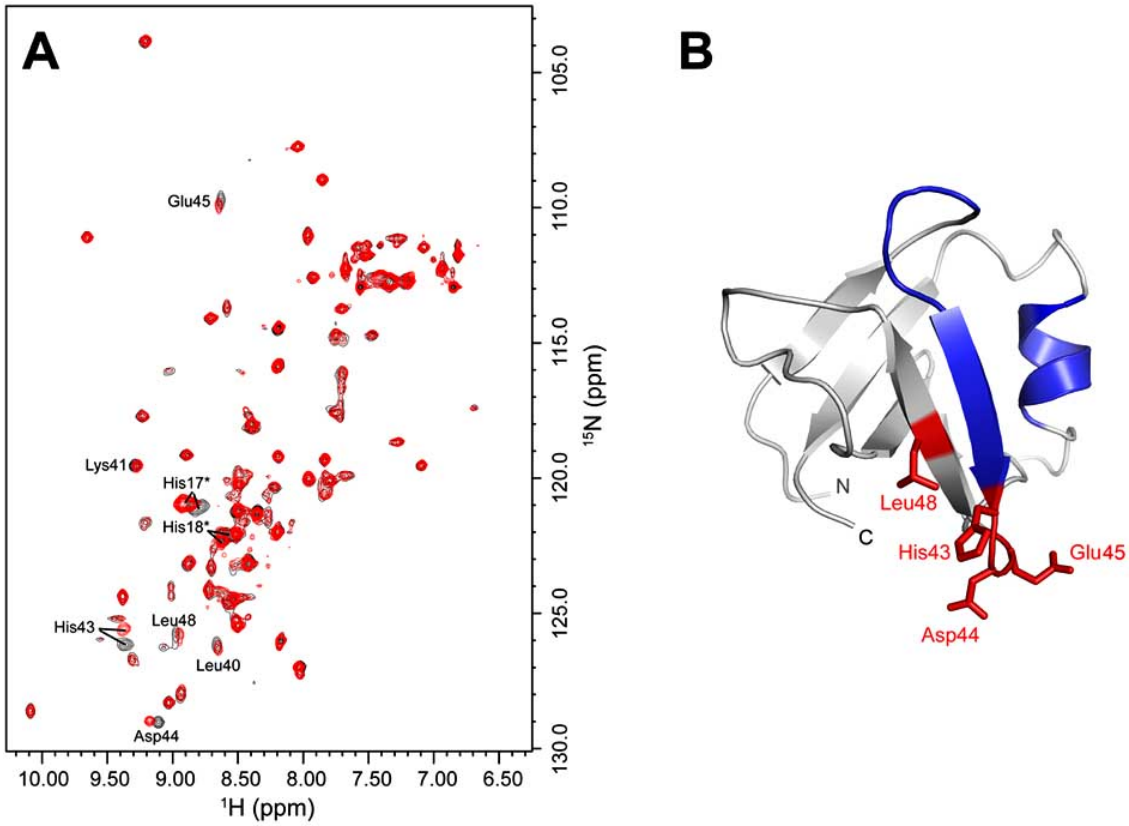

Figure 2. The interaction between the synbindin APD and the syndencan-2 cytoplasmic domain (S2CD). The His17* and His18* are belong to His_6-tag in the recombined protein for NMR experiments. **(A)** The overlay of ^{1}H-^{15}N HSQC spectra. Black, the ^{15}N labeled APD only. Red, the ^{15}N labeled APD with unlabeled S2CD (molar ratio 1:4). **(B)** Mapping the interaction site. Red, the interacting site indicated by NMR titration. Blue, the classical binding site of PDZ domain.

shift changes. With 0.4 mM APD, the S2CD:APD molar ratio reached to 4:1 can not saturate APD. Although further titration with higher S2CD concentrations is difficult because of the solubility, our NMR data indicated a weak binding with a K_D value larger than 1 mM.

Biological Implications of the Unique Binding Mode of the APD for Syndecan-2

As one of the most abundant protein module in eukaryotic genomes, PDZ domains act on protein targeting and protein complex assembly [27]. The interaction modes between PDZ domains and their ligands have been extensively studied [24,27]. The most prevalent bind mode of PDZ domains is to recognize a short peptide (less than 10 amino acid residues) situated at the extreme carboxyl terminus of a target protein. The key determinants of PDZ-binding carboxyl peptides are the residues at the 0 position (denoting the very last amino acid residue) and at the -2 position (the second residue N-terminal to the residue at the 0 position). The carboxyl group of the residue at the 0 position binds to the signature "Gly-ψ-Gly-ψ"-motif by forming hydrogen bonds with its backbone amides. In addition, the side-chain of the residue 0, which is often hydrophobic, inserts into the hydrophobic pocket formed at the one end of the αB and βB groove (corresponding $\alpha1_P$ and $\beta2_P$ in the APD). The side-chain of the residue at the -2 position interacts specifically with the first residue of αB, and this interaction largely determines the binding specificity between PDZ domains and its targets.

Synbindin was discovered as a syndecan-binding protein by interacting with the S2CD of syndecan, and the carboxyl "EFYA" sequence of syndecan-2 was shown to be essential for binding to synbindin [9]. Structural studies of synbindin and TRAPP subcomplex [28] reveled that synbindin contains a PDZ-like domain, the APD. However, in APDs of synbindin homologues, the "Gly-ψ-Gly-ψ"-motif was replaced by a conserved h-Asp-h motif ('h' standing for a hydrophobic residue) (Fig. **3** and Supp. Fig. **1**). Detailed structural analysis in previous [28] and current studies indicated that the APD lacks most important structural features for carboxyl peptide binding, and was suggested to be a protein-binding module interacting with an internal segment of a protein. This prediction was supported by our NMR based titration experiments, which show that the APD could only interact with the intact S2CD, but not with the S2CP (TKEFYA). The previous study reported that the syndecn-2 EFYA tail is essential for the synbindin APD binding, and therefore they concluded that APD interact with the syndecan-2 EFYA tail [9]. However, after the structure of synbindin was solved, we found that the APD used in previous study (residue number > 50 in human synbindin, Fig. **3**) lacks the first two β-strands and part of the third β-strand of the APD [9], while the second β-strand and the loop between the first two β-strands are the typical carboxyl-peptide bind-

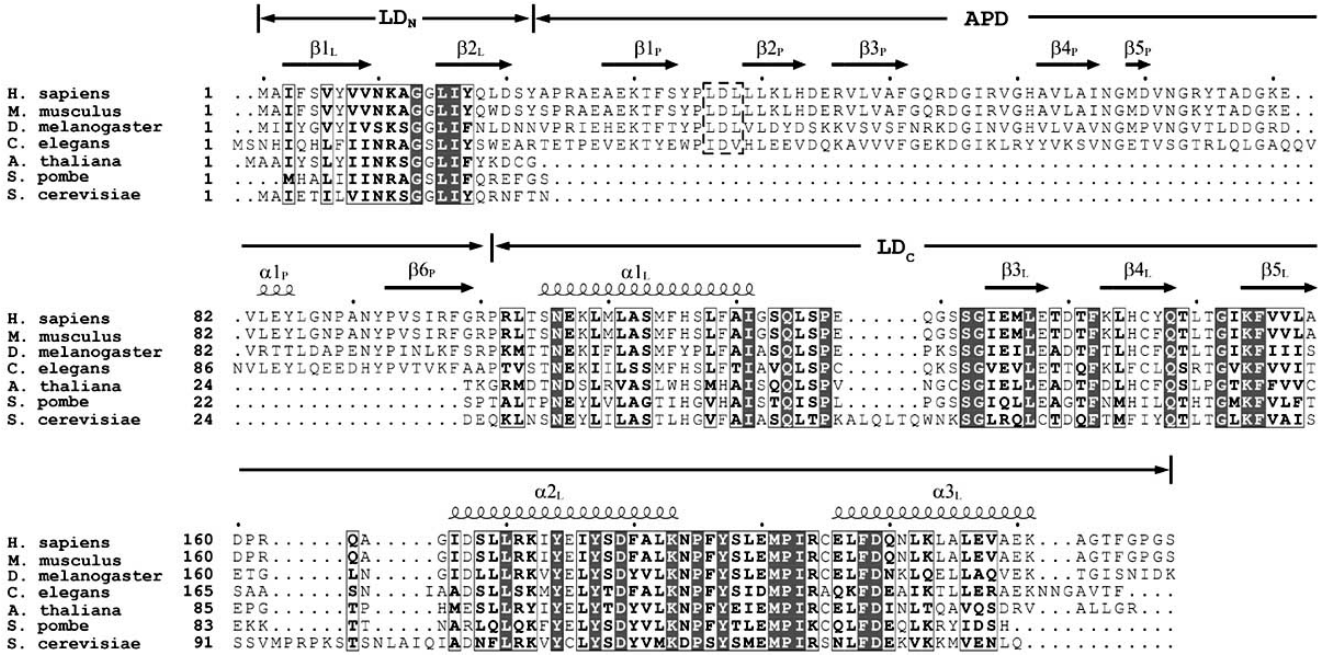

Figure 3. Multiple-sequence alignment of synbindins. The synbindin sequences of *Homo sapiens* (Human, Swiss-Prot accession number: Q9Y296), *Mus musculus* (Mouse, Q9ES56), *Drosophila melanogaster* (Fruit fly, Q9VLI9), *Caenorhabditis elegans* (Q20100), *Arabidopsis thaliana* (Q9LZ97), *Schizosaccharomyces pombe* (Fission yeast, O43041), and *Saccharomyces cerevisiae* (Baker's yeast, Q03784) are aligned using Tcoffee [29]. The secondary structures of human synbindin are indicated above the alignment diagram. The regions of LD_N, APD, and LD_C are labeled above the secondary structure. The conserved h-Asp-h motif ('h' standing for a hydrophobic residue) of the APD is dashed boxed.

ing site of PDZ-domains. Therefore, previous results are probably artifacts caused by the large change of protein surface and structure because of the missing ~1/3 part of the APD. Nevertheless, our data indicates the interaction between APD and syndecan-2 has a unique binding mode uncharacterized previously.

Although synbindin is one component of TRAPP complex, it may also have physiological role outside the complex. It is interesting to note that the APD is absent in Trs23, the yeast homolog of synbindin, suggesting that the function of the APD is unique in multicellular eukaryotes (Fig. **3**) [28]. Consistent with this notion, syndecan, a glycoprotein plays essential roles in cell adhesion and cell-cell signaling, does not exist in yeast. The APD domain in TRAPP I subcomplex structure have the freedom to move relative to the rest of the subcomplex [28]. In synbindin, APD inserted into a login domain (LD) sequence and make the longin domain into two parts: LD_N and LD_C. Analyzing sequences of the APDs from different organisms shows that the residues connecting the APD and LD_C or APD and LD_Ns are both highly conserved prolines (Fig. **3**), which may link with the large mobility of the APD. This mobility of the APD may be important for functional synbindin so that being retained during evolution. The interactions between synbindin APD and syndecan-2 reported here give the experimental evidences of the metazoan-specific protein-binding mode and may provide potential roles of synbindin outside the TRAPP complex.

ACKNOWLEDGEMENTS

This work is supported by Ministry of Science and Technology (Grant Nos. 2004CB720008, 2006CB0D1705), 863 program (2006AA02A316), the National Natural Science Foundation of China (Grant Nos 10490193 and 30721003) and the Chinese Academy of Sciences (KSCX2-YW-R-61). We thank Prof. Jinfeng Wang in Institute of Biophysics for NMR experiments.

ABBREVIATIONS

PDZ	=	PSD-95/Dlg/ZO-1 homology
TRAPP	=	Transport protein particle
LD	=	Longin domain
APD	=	Atypical PDZ domain
RMSD	=	Root mean square deviation
S2CD	=	The syndecan-2 cytoplasmic domain
S2CP	=	The syndecan-2 C-terminal peptide TKEFYA
HSQC	=	Heteronuclear single quantum coherence
DSS	=	Sodium 2,2-dimethylsilapentane-5-sulfonate

REFERENCES

[1] Sacher, M., Jiang, Y., Barrowman, J., Scarpa, A., Burston, J., Zhang, L., Schieltz, D., Yates, J.R., 3rd Abeliovich, H. and Ferro-Novick, S. TRAPP, a highly conserved novel complex on the cis-Golgi that mediates vesicle docking and fusion. (**1998**) *EMBO J.*, *17*, 2494-2503.

[2] Sacher, M., Barrowman, J., Wang, W., Horecka, J., Zhang, Y., Pypaert, M. and Ferro-Novick, S. TRAPP I implicated in the specificity of tethering in ER-to-Golgi transport. (**2001**) *Mol. Cell*, *7*, 433-442.

[3] Kummel, D., Muller, J.J., Roske, Y., Misselwitz, R., Bussow, K. and Heinemann, U. The structure of the TRAPP subunit TPC6 suggests a model for a TRAPP subcomplex. (**2005**) *EMBO Rep.*, *6*, 787-793.

[4] Turnbull, A.P., Kummel, D., Prinz, B., Holz, C., Schultchen, J., Lang, C., Niesen, F.H., Hofmann, K.P., Delbruck, H., Behlke, J., Muller, E.C., Jarosch, E., Sommer, T. and Heinemann, U. Structure of palmitoylated BET3: insights into TRAPP complex assembly and membrane localization. (**2005**) *EMBO J.*, *24*, 875-884.

[5] Kim, Y.G., Sohn, E.J., Seo, J., Lee, K.J., Lee, H.S., Hwang, I., Whiteway, M., Sacher, M. and Oh, B.H. Crystal structure of bet3 reveals a novel mechanism for Golgi localization of tethering factor TRAPP. (**2005**) *Nat. Struct. Mol. Biol.*, *12*, 38-45.

[6] Kim, M.S., Yi, M.J., Lee, K.H., Wagner, J., Munger, C., Kim, Y.G., Whiteway, M., Cygler, M., Oh, B.H. and Sacher, M. Biochemical and crystallographic studies reveal a specific interaction between TRAPP subunits Trs33p and Bet3p. (**2005**) *Traffic*, *6*, 1183-1195.

[7] Kummel, D., Muller, J.J., Roske, Y., Henke, N. and Heinemann, U. Structure of the Bet3-Tpc6B core of TRAPP: two Tpc6 paralogs form trimeric complexes with Bet3 and Mum2. (**2006**) *J. Mol. Biol.*, *361*, 22-32.

[8] Jang, S.B., Kim, Y.G., Cho, Y.S., Suh, P.G., Kim, K.H. and Oh, B.H. Crystal structure of SEDL and its implications for a genetic disease spondyloepiphyseal dysplasia tarda. (**2002**) *J. Biol. Chem.*, *277*, 49863-49869.

[9] Ethell, I.M., Hagihara, K., Miura, Y., Irie, F. and Yamaguchi, Y. Synbindin, A novel syndecan-2-binding protein in neuronal dendritic spines. (**2000**) *J. Cell. Biol.*, *151*, 53-68.

[10] Couchman, J.R. Syndecans: proteoglycan regulators of cell-surface microdomains?. (**2003**) *Nat. Rev. Mol. Cell. Biol.*, *4*, 926-937.

[11] Golovanov, A.P., Hautbergue, G.M., Wilson, S.A. and Lian, L.Y. A simple method for improving protein solubility and long-term stability. (**2004**) *J. Am. Chem. Soc.*, *126*, 8933-8939.

[12] Delaglio, F., Grzesiek, S., Vuister, G.W., Zhu, G., Pfeifer, J. and Bax, A. NMRPipe: a multidimensional spectral processing system based on UNIX pipes. (**1995**) *J. Biomol. NMR*, *6*, 277-293.

[13] Johnson, B.A. and Blevins, R.A. Nmr View - a Computer-Program for the Visualization and Analysis of Nmr Data. (**1994**) *J. Biomol. NMR*, *4*, 603-614.

[14] Herrmann, T., Guntert, P. and Wuthrich, K. Protein NMR structure determination with automated NOE assignment using the new software CANDID and the torsion angle dynamics algorithm DYANA. (**2002**) *J. Mol. Biol.*, *319*, 209-227.

[15] Duggan, B.M., Legge, G.B., Dyson, H.J. and Wright, P.E. SANE. (Structure Assisted NOE Evaluation): an automated model-based approach for NOE assignment. (**2001**) *J. Biomol. NMR*, *19*, 321-329.

[16] Cornilescu, G., Delaglio, F. and Bax, A. Protein backbone angle restraints from searching a database for chemical shift and sequence homology. (**1999**) *J. Biomol. NMR*, *13*, 289-302.

[17] Pearlman, D.A., Case, D.A., Caldwell, J.W., Ross, W.S., Cheatham, T.E., Debolt, S., Ferguson, D., Seibel, G. and Kollman, P. Amber, a Package of Computer-Programs for Applying Molecular Mechanics, Normal-Mode Analysis, Molecular-Dynamics and Free-Energy Calculations to Simulate the Structural and Energetic Properties of Molecules. (**1995**) *Comp. Phys. Commun.*, *91*, 1-41.

[18] Koradi, R., Billeter, M. and Wuthrich, K. MOLMOL: a program for display and analysis of macromolecular structures. (**1996**) *J. Mol. Graph.*, *14*, 51-55.

[19] Laskowski, R.A., Rullmannn, J.A., MacArthur, M.W., Kaptein, R. and Thornton, J.M. AQUA and PROCHECK-NMR: programs for checking the quality of protein structures solved by NMR. (**1996**) *J. Biomol. NMR*, *8*, 477-486.

[20] Holm, L. and Sander, C. Protein structure comparison by alignment of distance matrices. (**1993**) *J. Mol. Biol.*, *233*, 123-138.

[21] Krissinel, E. and Henrick, K. Secondary-structure matching. (SSM), a new tool for fast protein structure alignment in three dimensions. (**2004**) *Acta. Crystallogr. D Biol. Crystallogr.*, *60*, 2256-2268.

[22] Kang, B.S., Cooper, D.R., Jelen, F., Devedjiev, Y., Derewenda, U., Dauter, Z., Otlewski, J. and Derewenda, Z.S. PDZ tandem of human syntenin: crystal structure and functional properties. (**2003**) *Structure*, *11*, 459-468.

[23] Karthikeyan, S., Leung, T. and Ladias, J.A. Structural determinants of the Na+/H+ exchanger regulatory factor interaction with the beta 2 adrenergic and platelet-derived growth factor receptors. (**2002**) *J. Biol. Chem.*, *277*, 18973-18978.

[24] van Ham, M. and Hendriks, W. PDZ domains-glue and guide. (**2003**) *Mol. Biol. Rep.*, *30*, 69-82.

[25] Daniels, D.L., Cohen, A.R. Anderson, J.M. and Brunger, A.T. Crystal structure of the hCASK PDZ domain reveals the structural basis of class II PDZ domain target recognition. (**1998**) *Nat. Struct. Biol.*, *5*, 317-325.

[26] Grembecka, J., Cierpicki, T., Devedjiev, Y., Derewenda, U., Kang, B.S., Bushweller, J.H. and Derewenda, Z.S. The binding of the PDZ tandem of syntenin to target proteins. (**2006**) *Biochemistry*, *45*, 3674-3683.

[27] Hung, A.Y. and Sheng, M. PDZ domains: structural modules for protein complex assembly. (**2002**) *J. Biol. Chem.*, *277*, 5699-5702.

[28] Kim, Y.G., Raunser, S., Munger, C., Wagner, J., Song, Y.L., Cygler, M., Walz, T., Oh, B.H. and Sacher, M. The architecture of the multisubunit TRAPP I complex suggests a model for vesicle tethering. (**2006**) *Cell*, *127*, 817-830.

[29] Notredame, C., Higgins, D.G. and Heringa, J. T-Coffee: A novel method for fast and accurate multiple sequence alignment. (**2000**) *J. Mol. Biol.*, *302*, 205-217.

Received: June 08, 2008 Revised: August 04, 2008 Accepted: August 08, 2008